Radio Science, Volume 25, Number 5, Pages 825-836, September-October 1990

# Some comments on seabed propagation of ULF/ELF electromagnetic fields

Alan D. Chave

AT&T Bell Laboratories, Murray Hill, New Jersey

Agústa H. Flosadóttir and Charles S. Cox

Scripps Institution of Oceanography, La Jolla, California

(Received August 22, 1989; revised February 15, 1990; accepted February 16, 1990.)

A reference model for the electrical conductivity structure beneath the deep seafloor is proposed and justified using a variety of geophysical evidence. The model consists of relatively conductive sediment and crustal layers of 6.5 km extent overlying a resistive ($\approx 10^{-5}$ S/m) subcrustal channel of 30 km thickness and terminated in a deeper conductive layer and half-space. Its seafloor-to-seafloor response to a horizontal electric dipole source is explored as a function of frequency and range, showing that, compared with the response for a half-space with the lowest conductivity in the reference model, significant enhancement of the field amplitude can occur at long ranges (>100 km) and low frequencies (<1 Hz). At the same time, marked attenuation relative to the half-space response is seen at higher frequencies. The field enhancement is due to trapping of electromagnetic energy in a leaky subcrustal waveguide, as demonstrated by computing the complex Poynting vector. The attenuation occurs in the relatively conductive sedimentary and crustal layers overlying the lithospheric waveguide when their electrical thickness exceeds a skin depth. The results indicate that attempts either to model controlled electromagnetic sources or to interpret controlled source data using half-space models for the Earth can be badly misleading. The practicality of lithospheric communications in the real Earth is also investigated. Using measured receiver noise figures and the reference model, the receiver bandwidth necessary to achieve a given signal-to-noise ratio as a function of range and frequency is estimated for a seafloor horizontal source of strength $10^5$ A-m. The results indicate that significant ($\approx$100 km) ranges can be achieved only around 1 Hz with a bandwidth of $\approx$1 Hz at a SNR of 10, yielding a very low data rate of <3.5 bits/s. Longer ranges and higher frequencies are precluded by attenuation in the sediment and crustal layers and because the conductivity in the resistive channel is too large.

## INTRODUCTION

The propagation of electromagnetic waves through, under, and above the ocean from a submerged source in the ULF/ELF band (<3 kHz) is of potential interest in submarine communications and underwater detection. However, the attenuation (e-folding) scale of electromagnetic signals in seawater is quite small (270 m at 1 Hz) and decreases as the square root of the frequency. As a result, direct propagation through the sea has limited applications, and transmission mechanisms which increase the effective range become important. Recent theoretical investigations have focused on the "up-over-down" path through the atmosphere [e.g., Bubenik and Fraser-Smith, 1978; Fraser-Smith and Bubenik, 1979] and the "down-over-up" path along the relatively resistive seafloor [e.g., King et al., 1979; King and Brown, 1984;



Paper number 90RS00468.
0048-6604/90/90RS-00468$08.00

King, 1985a; Inan et al., 1986; Fraser-Smith et al., 1987, 1988], both of which involve the propagation of a surface-trapped or lateral wave along a horizontal interface between media of different electrical properties.

Electromagnetic propagation through subseafloor media also constitutes the basis for several geophysical exploration techniques. In the past decade, two practical methods that make use of seabed-to-seabed propagation have been developed for sounding the conductivity of the ocean floor; for a comprehensive review of this subject, see Chave et al. [1990]. The first seafloor technique is based on a vertical electric dipole (VED) source and horizontal magnetic field receivers [Edwards et al., 1981], and has been used for shallow sounding (to several kilometers) on the continental shelf and on the axis of a mid-ocean spreading center [Edwards et al., 1985; Nobes et al., 1986]. The second system employs a horizontal electric dipole (HED) source and horizontal electric field receivers, and is developed theoretically by Chave and Cox [1982a]. Experimental work based on this method is described by Young and Cox [1981] and Cox et al. [1986], and has yielded information about the electrical conductivity of the oceanic lithosphere to depths of 20 km or more. In particular, a relatively low conductivity ($\approx 10^{-5}$ S/m) region has been detected beneath the oceanic crust for moderate age lithosphere. New data on the shallower electrical structure of the oceanic crust are also available from dc and logging experiments conducted in boreholes. Taken together with information on the deep electrical conductivity of the Earth from magnetotelluric experiments, the results suggest marked vertical variation in the electrical conductivity beneath the oceans.

Most recent studies of seafloor-to-seafloor propagation, including those cited at the beginning of this paper, are based on half-space models for the Earth's electrical conductivity. Given our increasing knowledge about the electrical structure beneath the ocean and continuing interest in subseafloor propagation, it seems prudent to reexamine the problem using more realistic Earth models. In this paper, a reference model for the electrical conductivity structure of the oceanic lithosphere is proposed and justified using existing geophysical measurements. The model response for a near-bottom, time harmonic HED system is then explored as a function of frequency-range parameter space. Computations show that enhancement of the electric field amplitude by at least an order of magnitude over that for a half-space with the lowest conductivity in the model can occur at long ranges and low frequencies. At the same time, attenuation of the electric field by several orders of magnitude over that for a half-space is seen at higher frequencies. The former effect is due to energy trapping in a subcrustal low conductivity region, a conclusion which is confirmed by calculating the complex Poynting vector within the Earth. The attenuation at higher frequencies is due to dissipation in the relatively conductive oceanic crust and sediments overlying the resistive zone. These computations suggest that the interpretation of geophysical data using half-space models of the Earth is certain to be misleading. In particular, some conclusions of King et al. [1986] regarding the depth of penetration and ability of seafloor controlled source systems to sample deep structure are shown to be inapplicable in the presence of realistic subbottom layering. In addition, the potential for lithospheric communications is shown to be limited by the relatively conductive crust which separates the ocean from a low conductivity channel. To illustrate this, the paper closes by combining the computed signal levels for the reference model and realistic source moments with the measured noise level in the ULF/ELF electric field to estimate the receiver bandwidth necessary to reach a given signal-to-noise ratio as a function of range and frequency. The results indicate that significant ($\approx$100 km) ranges can be achieved only at around 1 Hz with a seafloor source unless extremely low data rates (<1 bit/s) are acceptable.

## ELECTRICAL STRUCTURE BENEATH THE SEAFLOOR

In the ocean and uppermost lithosphere that is of interest in this paper, the highest conductivity material likely to be encountered is ocean water. Seawater conductivity is roughly a linear function of in situ temperature, with a weaker pressure and salinity dependence, and varies from as much as 5 S/m near the surface to about 3.2 S/m below the main thermocline at 300-1000 m depth; the mean conductivity is about 3.2 S/m in the Pacific, with a slightly higher value applying in the Atlantic. A seawater conductivity profile at any location may easily be constructed using the empirical formulae contained in the work by Fofonoff and Millard [1983] together with historic average temperature and salinity information from Levitus [1982]. The mean depth of the oceans excluding the continental slopes and shelves is about 4.5 km, and outside of anomalous regions which account for a small percentage of its area, the depth range is 2.5–6 km. A well-determined relation between depth and the age of the underlying lithosphere based on a plate tectonic thermal cooling model explains most of the variation, so that young lithosphere is comparatively shallow.

Beneath the ocean layer, a variety of geophysical evidence suggests the division of the electrical lithosphere into four regions: sediments, the oceanic crust, the uppermost mantle, and the deep mantle. Three major factors control the electrical conductivity in these zones: water in fractures and pores at low temperatures (<600°C), thermally activated mineral mechanisms at higher but subsolidus temperatures, and the presence and connectedness of partial melt above the solidus. In the remainder of this section, the extent of the four subseafloor regions will be constrained based on geophysical data and an electrical conductivity model for them will be derived from field and laboratory measurements. Since displacement currents are completely negligible at the frequen-

cies of interest in this paper, the electrical permittivity structure will be ignored. However, it should be noted that the dielectric constant of seawater is about 80 while most oceanic rocks are not highly intrinsically polarizable; hence the permittivity structure of sediments and rock will depend largely on their water content.

The sediment layer is variable in thickness and has been mapped extensively using seismic reflection methods over the past several decades. Sediment is nearly absent at mid-ocean spreading centers and less than 100 m thick over vast tracts of the Pacific Ocean, while sediment blankets in excess of 1 km deep are seen in the abyssal plains of the Atlantic and Southern Oceans. Sediment thickness depends on several complex and interacting factors, including seafloor age, proximity of and connection to continental sources, biological productivity, chemical dissolution of biogenic components, and redistribution by bottom currents; for a review of this topic, see Kennett [1982]. The electrical conductivity of sediments depends on the presence of interstitial seawater, and hence on their porosity and degree of consolidation. The porosity of sediments is quite variable, but values in excess of 50% are usually seen in the uppermost 150 m, decreasing to 25% at 500 m, and 15-20% at 700 m [Tucholke et al., 1976]. These values can be combined with an empirical relation between porosity and electrical conductivity, Archie's law [Shankland and Waff, 1974], to predict a sediment conductivity profile. For unconsolidated, water-saturated sediments, the conductivity can approach that of seawater, while lithified material near the base of a thick sediment column may be two orders of magnitude more resistive. Because of the variable thickness of the sediment layer, the reference model will be divided into two types. The first will be called the Pacific model in which the sediment layer is absent, a condition which is reasonably representative of much of the eastern Pacific Ocean and lithosphere younger than a few million years elsewhere. The second case will be called the Atlantic model with a sediment layer 0.5 km thick having a conductivity of 0.3 S/m. The region below the sediments will be identical for both models. These two cases are intended only to illustrate the effect of a conductive sediment cap, and it should be remembered that both the thickness and conductivity of sediments may be variable.

Constraints on the structure of the oceanic crust are much stronger, primarily because it is remarkably uniform in space. The oceanic crust is usually divided into two regions on the basis of seismic experiments and field mapping of ophiolites (oceanic crust that has been emplaced on land): layer 2, a ≈1.5 km thick sequence of pillow basalts trending into sheet flows and terminated below by diabase dike complexes, and layer 3, a ≈5 km thick sequence of diabase dikes lying upon massive and cumulate gabbros. The relatively sharp Moho contact is reached at the base of the crust. The statistical uncertainty in crustal thickness is about 30%, although it is likely that most of the dispersion is due to difficulty in identifying and modeling seismic phases rather than to real variability. For a thorough description of the seismic and petrological structure of the oceanic crust, see Christensen and Salisbury [1975] or Spudich and Orcutt [1980].

Considerable information on the electrical conductivity of the oceanic crust is available from well logs and downhole dc resistivity experiments in Deep Sea Drilling Project boreholes. For Pacific crust, the conductivity in the top ≈0.6 km is highly variable because of changes in water content. In very young crust, the mean effective conductivity is ≈0.1 S/m, decreasing sharply to ≈0.002 S/m below this [Becker et al., 1982; Becker, 1985]. On old crust in the Atlantic, the mean effective conductivity is ≈0.03 S/m near the surface and shows a less marked decrease at depth [Becker, 1990]. Based on measurements in other boreholes, the overall conductivity appears to decrease with the age of the underlying lithosphere, probably due to crack sealing by chemical precipitates from hydrothermal activity and by reduction of the temperature of interstitial seawater. A decrease in conductivity with depth is also required by the data from three controlled source experiments [Young and Cox, 1981; Cox et al., 1986]. These observations lead to the following simplified model for ocean crustal electrical conductivity. In the upper layers, the conductivity is largely controlled by fractures, cracking, and the presence of seawater, varying with both the size and connectedness of fluid passages and fluid temperature. The reference model will have a 0.6 km thick layer of conductivity 0.03 S/m in this region; this conductivity value is a reasonable average of the observations and is uncertain by a factor of two. Beneath this point, the conductivity decreases in the low porosity dikes and massive gabbros. Since the intrinsic conductivity of the dry silicates making up the crust is ordinarily quite low, the bulk conductivity in layer 3 should be small (≈0.001 S/m), but may rise due to high temperatures in young crust. The reference model will include a 5.9 km thick layer of conductivity 0.003 S/m to account for this; the conductivity value is uncertain by a factor of 2 to 3. The conductivity structure discussed to this point is very similar to that originally proposed by Cox [1981].

Below the Moho, the electrical conductivity is expected to be much lower than in the crust because of reduced hydrothermal activity and a resulting low water content. Temperature has a controlling influence on conductivity if the volatile content is low, as shown by variations in the conductivity of dry gabbro between $10^{-5}$ S/m at 500°C and $10^{-2}$ S/m at 1000°C [Kariya and Shankland, 1983] and similar behavior at somewhat lower conductivities for peridotite [Constable and Duba, 1990]. Two controlled source electromagnetic studies over moderate age (25 Ma) lithosphere support these predictions, giving a conductivity of about $10^{-5}$ S/m in the uppermost lithosphere [Cox et al., 1986]. Unpublished data from a 1988 controlled source experiment also require highly resistive material below the crust. In addition, Wannamaker

et al. [1989] place an upper limit of $10^{-4}$ S/m on the conductivity of the uppermost lithosphere beneath the young Juan de Fuca plate off of the Pacific Northwest, and Mackie et al. [1988] could not explain land electromagnetic observations in California at periods of 1–30 h without invoking a zone of low conductivity material beneath the nearby ocean. None of these data strongly constrain an expected rise in conductivity due to increasing temperature at depth. However, laboratory data and mantle geotherms indicate that conductivity will grow quickly below 30 km [Constable and Duba, 1990]. These data also suggest that changes in mantle conductivity with lithospheric age will be substantial. Figure 1 is a cartoon that summarizes the pertinent results. Some of the details in Figure 1 are speculative, especially the age dependence of the mantle low conductivity zone and its depth extent, but the trends are reasonably well established.

The mantle part of the reference model includes a 30 km thick layer of conductivity $10^{-5}$ S/m representative of moderate age lithosphere. Beneath this layer, a 40 km thick zone of 0.003 S/m conductivity overlying a half-space of conductivity 0.1 S/m is included to crudely simulate the increase in conductivity with temperature at depth and yield agreement with oceanic magnetotelluric data [e.g., Oldenburg et al., 1984]. The model conductivities are probably accurate to within a factor of 2 to 3, while the thickness of the subcrustal resistive layer is not likely to vary by more than 50%. The lateral extent of the resistive layer is far more uncertain. The resistive zone is not expected to be present everywhere in the ocean basins; in particular, near mid-ocean spreading centers high temperatures will lead to larger conductivities (see Figure 1) and subduction zones can provide conductive pathways to the deeper interior of the Earth as observed off Oregon by Wannamaker et al. [1989]. In addition, virtually all magnetotelluric data from the deep ocean display only weak anisotropy, indicating that a predicted continental edge polarization effect that is exacerbated by a low conductivity mantle layer [Cox, 1980] has a limited effect and suggesting the presence of conductive pathways to the deep mantle in many parts of the ocean basins.

The model proposed and justified in this section has general validity in the deep ocean over moderate age lithosphere, but is not intended to represent the conductivity structure of continental margins even approximately. The margins are a transitional region toward a continental structure with a crust that is 6-7 times thicker than the oceanic value. Continental margins typically contain much more extensive sedimentary sequences than are seen in the open ocean. While no data comparable to the controlled source results for the margins are currently available, it is expected that more conductive material will exist immediately beneath the seafloor, restricting the range of ULF/ELF propagation from a submerged source over the deep ocean value. Information on shallow electrical connections between land and the offshore oceanic lithosphere is also lacking; a single attempt to detect one in a geologically atypical area failed [Bostick et al., 1978].

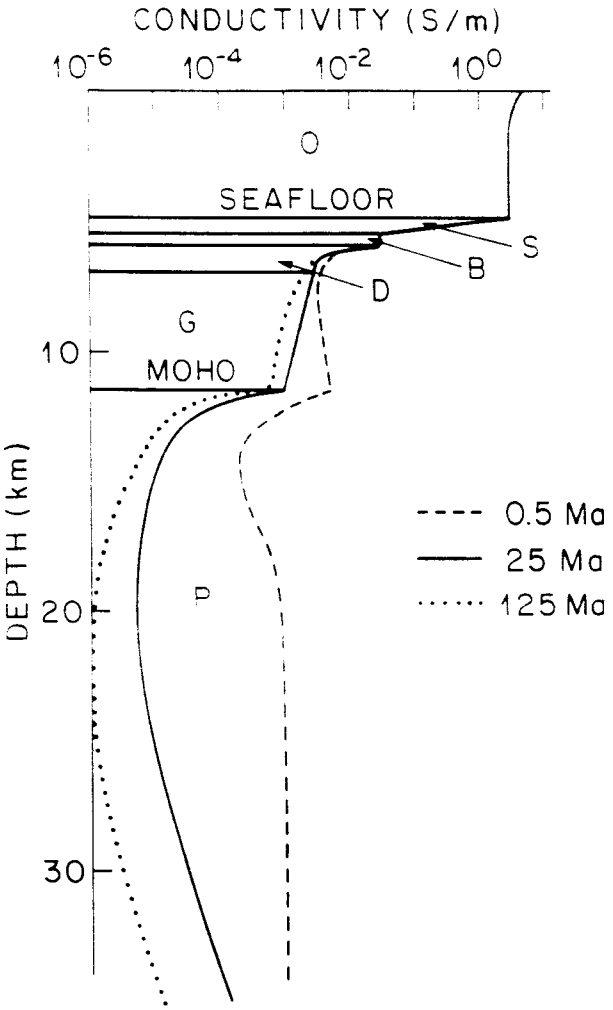


Fig. 1. Cartoon showing the variation in electrical conductivity from the sea surface to a depth of about 40 km beneath the seafloor for lithosphere of age 0.5 Ma (dashed line), 25 Ma (solid line), and 125 Ma (dotted line). The different vertical zones are discussed in the text, and include the ocean (O), sediments (S), pillow basalts (B), diabase sheeted flows (D), massive and cumulate gabbros (G), and mantle peridotite (P). The 25 Ma curve is the most strongly constrained by existing measurements and is discussed in the text.

Figure 2 and Table 1 summarize the two versions of the reference model for the electrical conductivity beneath the deep seafloor.

## EFFECT ON THE HED ELECTRIC FIELD

Virtually all recent model studies of subsurface-to-subsurface propagation treat the electrical structure beneath

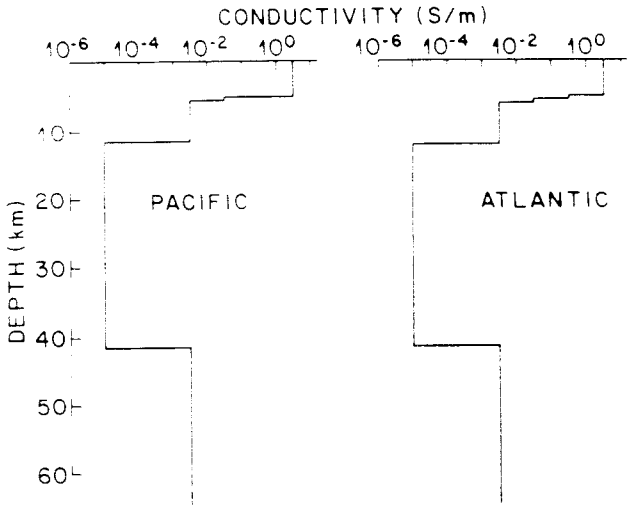


Fig. 2. Layered approximations to Figure 1 that constitute the reference model for the sediment-free Pacific case (left) and the sediment-capped Atlantic case (right). Both models are terminated in a half-space of conductivity 0.1 S/m below 76.5 km depth. See text for details.

the seafloor as a half-space, either because approximate analytic formulae for the electromagnetic fields can be obtained [e.g., King and Brown, 1984; King, 1985a] or to simplify numerical computations [e.g., Fraser-Smith et al., 1987, 1988]. Bannister [1984] has recently reexamined the analytic formulae used by King and coworkers, relating them to earlier results summarized by Kraichman [1970], establishing the range of parameter space where they are valid more precisely, and correcting some errors. He also identifies three parts of the wave field in the ocean: a direct part propagating away from the source, a modified mirror image of the source, and a lateral or surface-trapped wave propagating along the interface. The latter is the dominant component of the wave field near the seafloor at ranges in excess of a few times the skin depth in seawater when the underlying medium is a half-space. However, interface waves constitute an important part of the physics within layered media as well as along the seafloor, as will be evident in the numerical simulations contained in this paper.

TABLE 1. Reference Conductivity Model

| Pacific | | Atlantic | |
|---|---|---|---|
| Thick., km | Cond., S/m | Thick., km | Cond., S/m |
| 4.5 | 3.2 | 4.5 | 3.2 |
| 0.0 | 0.0 | 0.5 | 0.3 |
| 0.6 | 0.03 | 0.6 | 0.03 |
| 5.9 | 0.003 | 5.9 | 0.003 |
| 30 | 0.00001 | 30 | 0.00001 |
| 40 | 0.003 | 40 | 0.003 |
| ∞ | 0.1 | ∞ | 0.1 |

It is well known that a horizontal source in a conductive region couples to a resistive medium more efficiently than a vertical one. As a consequence, the seafloor horizontal electric field produced by an infinitesimal, time-harmonic, horizontal electric dipole of unit (1 A-m) moment lying at the ocean bottom will be considered in this paper using the reference model for electrical conductivity (except that the ocean layer is replaced by a half-space). Chave and Cox [1982a] have derived formulae for the electromagnetic fields produced by infinitesimal horizontal and vertical electric dipole sources in a finite depth ocean above an arbitrary layered Earth. The expressions from this study are exact except that displacement current effects have been ignored, and do not neglect either the lateral wave terms, as suggested by King [1985a] and King et al. [1986], or any other significant part of the wave field. The numerical evaluation of the resulting Hankel transform expressions is accomplished rapidly and accurately using direct quadrature augmented by a Padé approximant convergence acceleration step as given by Chave [1983].

Using this approach, Figure 3 compares the radial electric field at zero azimuth (i.e., the component in the direction of the source dipole) as a function of range at four frequencies for the Atlantic and Pacific reference models with that for a half-space of conductivity $10^{-5}$ S/m. This conductivity value is the minimum one in the reference model of Figure 2 and Table 1, and will result in a lower attenuation rate with distance from a dipole source than any higher conductivity. The half-space field in Figure 3 decays monotonically with range at a rate which increases with frequency and is dominated by the interface wave component at all distances in excess of a few skin depths in seawater; this is 2.7 km, 900 m, 270 m, and 90 m respectively at the four frequencies shown. For comparison purposes, a skin depth in $10^{-5}$ S/m material is 1600 km, 500 km, 160 km, and 50 km at the same four frequencies. At low frequencies (<1 Hz), the reference model response displays a strong enhancement of the field amplitude at all ranges beyond ≈100 km with the difference between the model and half-space responses increasing as a function of source-receiver distance. At 1 Hz, the reference model and half-space solutions are less distinct than at 0.01 and 0.1 Hz. At all ranges, the Atlantic model has a slightly lower amplitude than the Pacific one due to the attenuating effect of the sediment layer. At 10 Hz (and for higher frequencies), the reference model response is much weaker than the half-space one, typically by a decade or more, and the Atlantic model is markedly more attenuated than the Pacific one. However, the reference model electric field decays with range at the same rate as the half-space response once distances exceed a few tens of kilometers.

Further insight can be obtained by examining the time averaged flow of energy for the Pacific reference and half-space models. For a layered model, this is most easily accomplished in an asymptotic long range limit using the

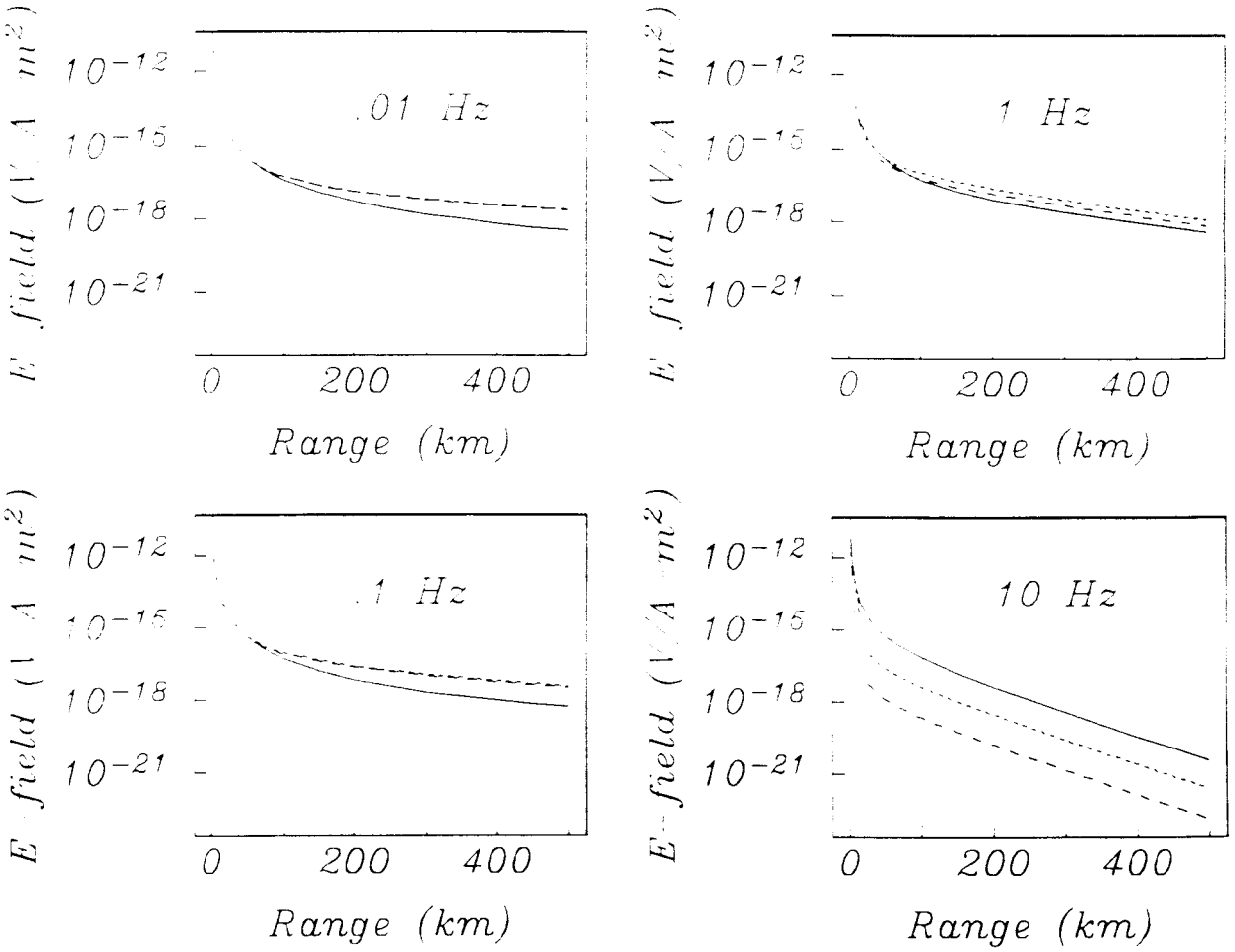


Fig. 3. The amplitude of the seafloor electric field per unit source moment in the direction of the source dipole as a function of source-receiver range at 0.01, 0.1, 1, and 10 Hz. The solid line is the response for a half-space of conductivity $10^{-5}$ S/m, while the Pacific and Atlantic reference model responses are shown by the short- and long-dashed lines respectively.

least attenuated term in an eigenmode expansion to represent the electromagnetic fields [Flosadóttir, 1990]. This approach is preferred because of inherent numerical difficulties with the direct evaluation of Hankel transform expressions for the fields at depth in a layered model. The eigenmode calculation is appropriate for the underwater problem at frequencies high enough for the ocean and deep mantle to form electrically thick barriers such that signals originating at the seafloor cannot propagate into the atmosphere or to great depths in the Earth. In this limit, the artifice of placing perfectly conducting boundaries at the sea surface and deep in the Earth is justified, confining the response to a discrete set of modes. To quantify this, Figure 4 compares the seafloor electric fields for the Pacific reference model using the lowest eigenmode and direct numerical integration. After higher modes have decayed to negligible levels (beyond 100 km at 0.1 Hz), the two are in agreement to a few percent which is adequate for present purposes.

Figure 5 shows the time-averaged flow of energy for the Pacific reference and half-space models in a vertical cross section through the ocean and seafloor containing the source dipole. The flux arrows are presented starting from the range where the exponential decay undergone by the second mode relative to the first one has exceeded a factor of 100, so that at all longer ranges the first mode dominates the electromagnetic field. The arrows are the tangents to the real part of the complex Poynting vector which is interpreted as the time-averaged (over a complete period of the source) energy flux; they have been drawn reflecting the vertical exaggeration in the figure and have lengths which vary logarithmically with the time-averaged energy flux magnitude over a range of ten decades, full scale being set arbitrarily at

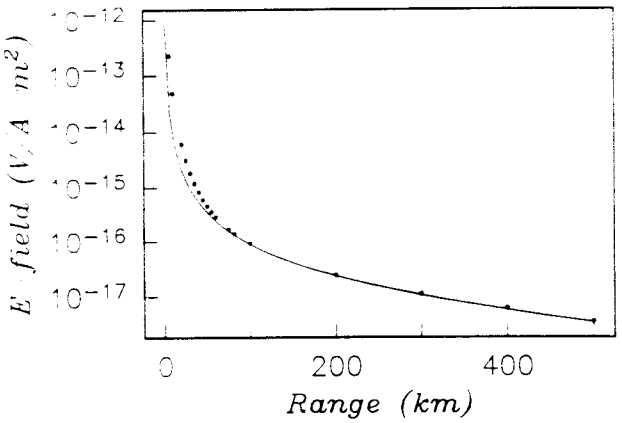


Fig. 4. The amplitude of the seafloor radial electric field per unit source moment for the Pacific reference model at 0.1 Hz computed using direct numerical integration (solid dots) and the lowest order term in the eigenmode expansion described in the text (solid line). After higher modes have decayed to negligible levels at about 100 km range, the two methods are in reasonable agreement.

the largest arrow presented in each plot. The lower panels show the flux tangents for a half-space of conductivity $10^{-5}$ S/m calculated numerically using Hankel transform expressions for the electric and magnetic fields. It is clear that the Pacific model response (upper panels) is dominated by horizontal energy flow in the low conductivity zone with leakage both into the deeper mantle and into the crust occurring at all ranges shown. By contrast, the half-space result (lower panels) is dominated by flow along the seafloor-rock interface, although energy loss by propagation into the Earth and in the conductive ocean is evident.

A qualitative understanding of the main features in Figure 3 is easily gained by considering the subcrustal low conductivity channel in Figure 2 as a leaky waveguide that is separated from the source by a relatively high attenuation region (the sediments and crust), an idea developed by Wait [1954], Wheeler [1961], Mott and Biggs [1963], Wait [1966], and others in analogy with the Earth-ionosphere waveguide. At low frequencies the sediment and crustal region is only a fraction of a skin depth thick and has little effect, but the presence of the resistive channel between the

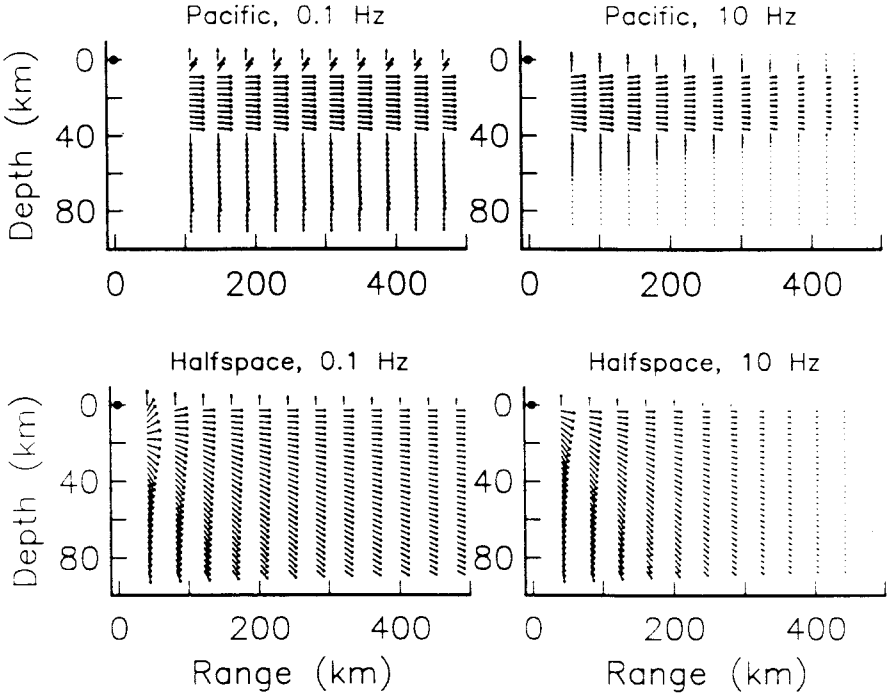


Fig. 5. Tangents to the time-averaged energy flux in a vertical section (where zero depth corresponds to the seafloor) containing a source HED at the seafloor as indicated by the solid circle. The energy flux is given by the real part of the complex Poynting vector $\vec{S}=(\vec{E}\times\vec{H}^{*})/2$. The arrow directions reflect the vertical exaggeration and their lengths are scaled logarithmically over ten decades. Full scale corresponds to 27 km on the horizontal axis and is set at the maximum value for the energy flux in each plot. The upper panels show the time-averaged energy flux for the Pacific reference model at 0.1 Hz and 10 Hz in the long range limit represented by the first term in a modal expansion (see text). The lower panels show the same quantity for a $10^{-5}$ S/m half-space.

crust and deeper mantle provides a low attenuation path for electromagnetic signals. Beyond a minimum distance of ≈75 km, the bottom of the waveguide begins to be evident and trapping becomes significant. At frequencies slightly above 1 Hz the physical thickness of the sediment and crustal region becomes roughly an electromagnetic skin depth. At 1 Hz, attenuation relative to the half-space occurs at short ranges (<75 km) where the waveguide bottom is not felt, while at longer ranges the enhancement due to waveguide trapping is less pronounced than for lower frequencies. At 10 Hz and above, the sediment and crustal layers are quite important and attenuation in the down and up parts of the path is severe. The waveguide bottom has a limited influence on propagation because the thickness of the resistive zone is comparable to a skin depth, but an interface wave does propagate along the crust-mantle boundary as evidenced by the similar asymptotic slopes of the model and half-space responses.

The validity of the lithospheric waveguide interpretation is further established by comparing Figure 3 with the response of a model in which the conducting layers below the reference model's resistive zone have been removed, extending the low conductivity region to infinity (Figure 6). The low frequency enhancement of the field amplitude relative to the half-space value has now vanished, and as the frequency rises above 1 Hz, the sediment and crustal layers simply increase the attenuation. The trapping seen in Figure 3 is only a weak function of the thickness of the resistive zone: halving its extent produces a slight enhancement of the field amplitude at all ranges and a small decrease in the distance

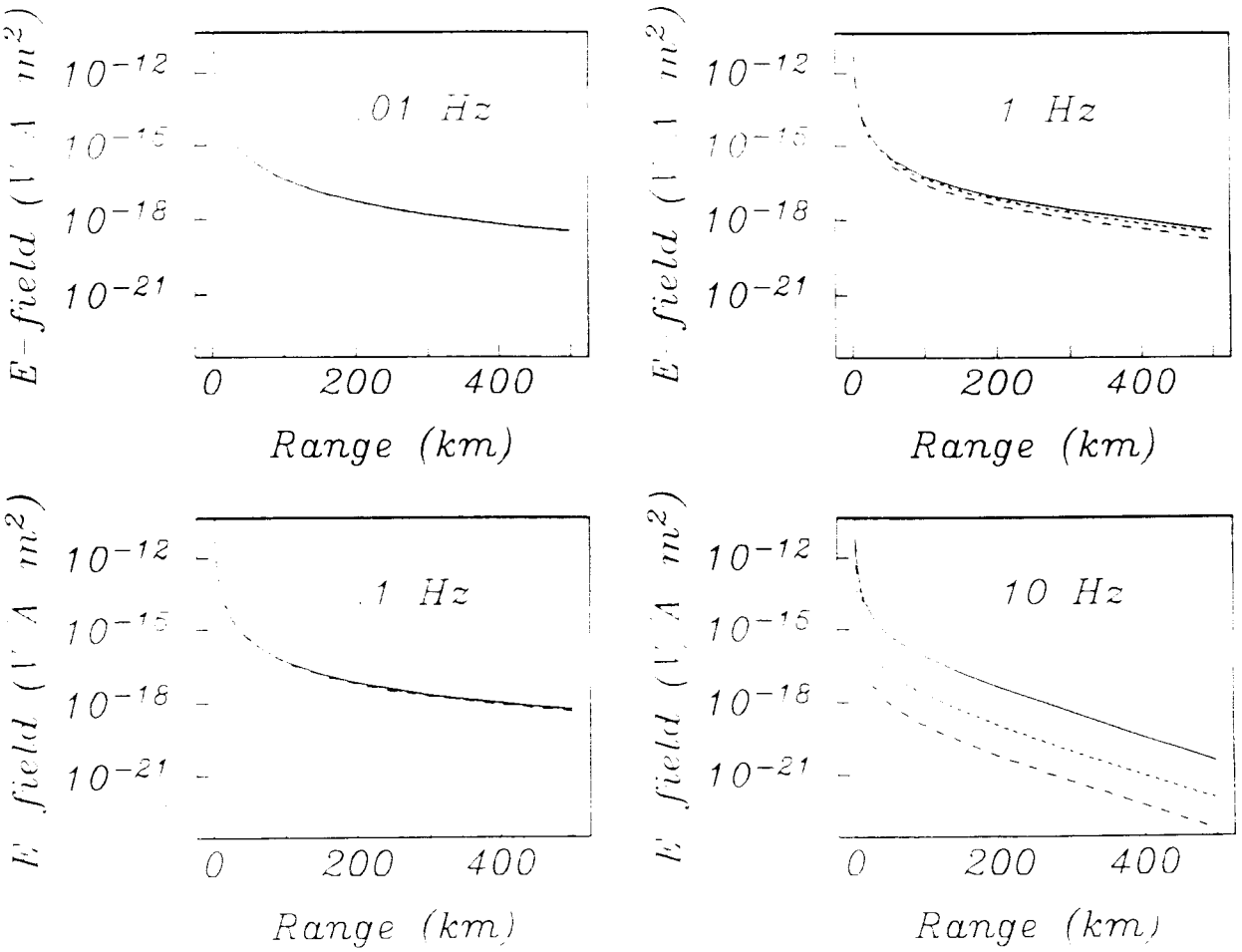


Fig. 6. The amplitude of the electric field per unit source moment in the direction of the source dipole as a function of source-receiver range at 0.01, 0.1, 1, and 10 Hz. The solid line is the response for a half-space of conductivity $10^{-5}$ S/m, while the short- and long-dashed lines show the Pacific and Atlantic reference models except that the low conductivity zone beneath the crust is extended to infinity, eliminating the deep conductivity increase.

where waveguide trapping becomes significant. Increasing its thickness weakens the trapping effect, as seen for the ultimate limit in Figure 6. Trapping depends more strongly on the conductivity in the channel; an increase by a factor of ten results in a large reduction in field amplitude with increasing range.

No attempt has been made in this paper to model the "up-over-down" path through the air, although its inclusion in the computations of Figures 3 and 6 is straightforward. This propagation mode is of little importance for sources and receivers located near the floor of the real ocean at frequencies above 0.01 Hz at useful ranges. To see this, note that the depth range of the ocean is $4.5 \pm 2$ km, while a skin depth in seawater ranges from 2.7 to 0.09 km over the 0.01-10 Hz band. It is only at the lowest frequencies and longest ranges in water shallower than is typical of the open ocean that this propagation mode will even be weakly manifest. This argument clearly breaks down when the source and receiver are located near the sea surface; see Fraser-Smith et al. [1987] for an elaboration.

## DISCUSSION

From the examples given here, it should be clear that the use of simple half-space approximations for the conductivity beneath the seafloor can lead to substantial errors in estimating the amplitude and phase changes as a function of either frequency or range for an HED source in the real ocean. Similar calculations can easily be carried out for other source and receiver combinations and will yield similar conclusions. In preference to half-space models, it is recommended that the reference model presented in this paper be adopted when actual field behavior is of interest since it represents a synthesis of current information on seafloor conductivity. At the same time, the limitations of the reference model must be borne in mind; there is no universal model for the electrical conductivity structure beneath the seafloor. Because of the known spatial variability of sediment thickness in the world oceans and probable correlation of the conductivity and thickness of the subcrustal resistive channel with lithospheric age, it is necessary to examine marine geologic and tectonic information carefully to ensure that the reference model is applicable in a given location or to guide modifications. In particular, it should be remembered that the structure of the continental margins and shelves will be markedly different from that of the reference model.

In an early study, Young and Cox [1981] employed numerical modeling to show that an ensemble of the best fitting layered models to a set of seafloor HED data require a decrease in conductivity beneath the oceanic crust. In several recent papers, King [1985a,b], Pan [1985], and Brown and King [1986] have attempted to use analytical formulae for the electromagnetic fields due to a point HED source at the interface between two conducting half-spaces to reinterpret these results. There are at least two reasons why this is not prudent. First, these data were collected at a single source-receiver range of ≈20 km and for a limited set of frequencies. Figure 3 shows that differences between layered and half-space models are not well developed at short ranges where the subcrustal layers are not sampled adequately. The distinction between a layered and a half-space model fit to a set of data is correspondingly subtle and potentially difficult to discern in the presence of noise. The more extensive data set described in Cox et al. [1986] includes ranges to 70 km from the source and a larger number of frequencies, and cannot be fit adequately by a half-space model. Second, it is well known that an infinite number of models can be generated which match a set of noisy data with comparable misfit, so that side constraints based on resolution, regularization, or other data must be imposed to limit the dimensionality of the model space. In addition, it is not adequate merely to fit a model to a set of data; the uncertainty of the model must also be assessed as completely as possible. These ideas lie at the heart of the formalism of geophysical inverse theory [e.g., Parker, 1977]. The imposition of a half-space structure is a very strong constraint on the class of models that can be fit to a set of data. Estimates of data resolution and model uncertainty made subject to such a constraint will not be very relevant to the real Earth.

In another study, King et al. [1986] derived analytical expressions for the complex Poynting vector due to an HED source in a medium consisting of two conducting half-spaces and estimated the effect of a perfectly reflecting surface at depth. They concluded that the lateral wave part of the field sampled only a relatively thin layer beneath the ocean and constituted 60-90% of the observed electromagnetic field at the seafloor. However, this calculation has no relevance to layered structures containing buried resistive zones such as the reference model where the dominant energy flux occurs within the Earth, not at the seafloor. This is graphically illustrated by Figure 3 and the top panels of Figure 5. Any interface wave present at the seafloor-rock junction is weak by comparison to the trapped wave in the subcrustal resistive zone. Figure 6 shows that the dominant wave field component at long range can be an interface wave along a subseafloor boundary even when a waveguide structure is not evident. This indicates that it is important to model all relevant components of the wavefield when computing seafloor controlled source electromagnetic fields, including the seafloor lateral wave, deeper interface waves, and incident or reflected space waves, as was done by Young and Cox [1981], Chave and Cox [1982a], and Cox et al. [1986]. In particular, the conclusion of King et al. [1986] that most of the energy flow occurs just beneath the seafloor appears to have misled King [1985b], Pan [1985], and Brown and King [1986] into believing that HED fields can only sample the uppermost few hundred meters of the

seafloor, justifying the use of analytic formulae for geophysical interpretation. Great care must be taken not to attribute too much importance to the lateral wave component at the seafloor. Ignoring the part of the wavefield flowing at depth can lead to large errors in interpretation.

Since the early days of interest in lithospheric communications, the general lack of information about conductivity beneath the seafloor has been deplored [e.g., Mott and Biggs, 1963; Fraser-Smith et al., 1988]. A clearer picture has begun to emerge from experimental work over the past decade, as summarized in the reference model, and realistic evaluation of conjectures about long range propagation of electromagnetic waves in the oceanic lithosphere is possible for the first time. By combining the calculations of Figure 3 with some practical characteristics of sources and receivers, it is possible to estimate the bandwidth required to realize a given signal-to-noise ratio as a function of source-receiver range using the reference conductivity model. This can be applied to computing the maximum range over which data might be transmitted in the real ocean. A number of assumptions must be made to achieve this. First, the source moment will be taken as $10^5$ A-m, corresponding to a source dipole 1 km long carrying 100 A of current; this is comparable to that of the system used by Cox et al. [1986]. Accounting for ohmic losses between a surface generator and the seabed, this would require about 10 kW of power, and significant increases can be achieved only at great expense, especially if the source is submerged. Second, the receiver dipole will be assumed to have a length of 1 km, similar to those described by Webb et al. [1985]. Longer antennae can be deployed only with difficulty, and their extent is ultimately limited by the effect of signal phase differences along the antenna as well as phase variations caused by conductivity inhomogeneity of the seafloor. Third, experience has shown that conductive coupling of the receiver to the ocean can best be accomplished using Ag-AgCl electrodes. Based on Webb et al. [1985], the dominant sources of receiver noise are due to electrochemical effects in the Ag-AgCl electrodes at frequencies above 0.5 Hz and ionospheric and microseismic sources at lower frequencies.

The power signal-to-noise ratio for a sinusoidal source is given by

$$SNR = \frac{A^2}{4S_n\Delta f} \tag{1}$$

where $A$ is the source amplitude at the receiver given in Figure 3, $S_n$ is the receiver noise spectral density given by Webb et al. [1985, Figure 7], and $\Delta f$ is the receiver bandwidth. Choosing a target signal-to-noise ratio of 10, (1) is easily solved for $\Delta f$. The results at the four frequencies of Figure 3 and at ranges of 100, 300, and 500 km are shown in Table 2. It is clear that extremely small bandwidths are necessary except at ranges below 100 km at around 1 Hz. Since the medium is dispersive, the usable bandwidth could be further limited as discussed by Inan et al. [1986]. The phase difference across a 1 Hz band centered at 1 Hz is about 20° at 100 km and 100° at 300 km, so dispersion is not a serious limitation at the shorter range. This suggests that seafloor-to-seafloor propagation might be of practical use for communications over ranges of 100 km or less in the deep ocean. Even if a SNR as low as 1 is acceptable, the resulting bandwidth is too small for useful communications at other frequencies. However, the data rate that can be achieved even at 1 Hz is extremely small. To see this, assume that SNR is constant across a 1 Hz band centered at 1 Hz and compute the maximum average data rate [Raemer, 1969, chapter 3]

$$C = \Delta f \log_2(1+SNR) \tag{2}$$

yielding a value of ≈3.5 bits/s at an SNR of 10. This is probably an overestimate by at least a factor of two because of the expected rapid variation in SNR with frequency and dispersion effects. This suggests that a 100 bit message would require of order a minute to send without allowing for error checking. Higher data rates can be achieved only by increasing the frequency, but this is prohibited by the relatively conductive sediments and crust. Similarly, longer ranges at low frequency cannot be reached unless the subcrustal conductivity is dramatically lower than has been measured. Based on laboratory data on silicate rock conductivity and geophysically inferred mantle geotherms, this is unlikely. Even emplacing both source and receiver in boreholes through the most conductive parts of the sediments and crust offers only limited improvement unless extremely deep penetration can be achieved [Chave and Cox, 1982b], and will be limited to the comparatively inefficient vertical electric dipole system. Since about six months of drill ship time was required to penetrate ≈1.5 km of ocean crust at Deep Sea Drilling Project Hole 504B, the deepest hole

TABLE 2. Receiver Bandwidth Versus Frequency and Range at SNR=10

| f, Hz | 100 km | 300 km | 500 km |
|---|---|---|---|
| 0.01 | $7.8\times10^{-5}$ | $9.6\times10^{-7}$ | $1.4\times10^{-7}$ |
| 0.1 | 0.042 | $6.1\times10^{-4}$ | $6.5\times10^{-5}$ |
| 1 | 1.5 | 0.086 | $1.8\times10^{-4}$ |
| 10 | 0.021 | $9.1\times10^{-7}$ | $8.5\times10^{-7}$ |

beneath the ocean to date, a borehole approach is also costly. Thus, the sort of long range, secure lithospheric communications system envisioned by Wheeler [1961] or Mott and Biggs [1963] does not appear practical.

## REFERENCES


Bannister, P. R., New simplified formulas for ELF subsurface-to-subsurface propagation, *IEEE J. Oceanic Eng., OE-9*, 154–163, 1984.

Becker, K., Large-scale electrical resistivity and bulk porosity of the oceanic crust, Deep Sea Drilling Project Hole 504B, Costa Rica Rift, *Initial Rep. Deep Sea Drill. Proj., 83*, 419–427, 1985.

Becker, K., Large-scale electrical resistivity and bulk porosity of the upper oceanic crust at Hole 395A, *Proc. Ocean Drill. Prog.: Sci. Results, 106/109*, 205–212, 1990.

Becker, K., R. P. Von Herzen, T. J. G. Francis, R. N. Anderson, J. Honnorez, A. C. Adamson, J. C. Alt, R. Emmerman, P. D. Kempton, H. Kinoshita, C. Laverne, M. J. Mottl, and R. L. Newmark, In situ electrical resistivity and bulk porosity of the oceanic crust, Costa Rica Rift, *Nature, 300*, 594–598, 1982.

Bostick, F. X., C. S. Cox, and E. C. Field, Jr., Land-to-seafloor electromagnetic transmissions in the 0.1 to 15 Hz band, *Radio Sci., 13*, 701–708, 1978.

Brown, M. F., and R. W. P. King, Shallow sounding of crustal regions using electromagnetic surface waves, *Radio Sci., 21*, 831–844, 1986.

Bubenik, D. M., and A. C. Fraser-Smith, ULF/ELF electromagnetic fields generated in a sea of finite depth by a submerged vertically-directed harmonic magnetic dipole, *Radio Sci., 13*, 1011–1020, 1978.

Chave, A. D., Numerical integration of related Hankel transforms by quadrature and continued fraction expansion, *Geophysics, 48*, 1671–1686, 1983.

Chave, A. D., and C. S. Cox, Controlled electromagnetic sources for measuring electrical conductivity beneath the oceans, 1, forward problem and model study, *J. Geophys. Res., 87*, 5327–5338, 1982a.

Chave, A. D., and C. S. Cox, On the use of boreholes in controlled electromagnetic source soundings of the ocean crust, *Ref. 82-24*, 39 pp., Scripps Inst. of Oceanogr., La Jolla, Calif., 1982b.

Chave, A. D., S. C. Constable, and R. N. Edwards, Electrical exploration methods for the seafloor, *Electromagnetic Methods in Applied Geophysics*, vol. 2, edited by M.N. Nabighian, Society of Exploration Geophysicists, Tulsa, Okla., in press, 1990.

Christensen, N. I., and M. H. Salisbury, Structure and constitution of the lower oceanic crust, *Rev. Geophys., 13*, 57–86, 1975.

Constable, S. C., and A. G. Duba, Electrical conductivity of olivine, a dunite, and the mantle, *J. Geophys. Res. 95*, 6967–6978, 1990.

Cox, C. S., Electromagnetic induction in the oceans and inferences on the constitution of the Earth, *Geophys. Surv., 4*, 137–156, 1980.

Cox, C. S., On the electrical conductivity of the oceanic lithosphere, *Phys. Earth Planet. Inter., 25*, 196–201, 1981.

Cox, C. S., S. C. Constable, A. D. Chave, and S. C. Webb, Controlled-source electromagnetic sounding of the oceanic lithosphere, *Nature, 320*, 52–54, 1986.

Edwards, R. N., L. K. Law, and J. M. DeLaurier, On measuring the electrical conductivity of the oceanic crust by a modified magnetometric resistivity method, *J. Geophys. Res., 86*, 11609–11615, 1981.

Edwards, R. N., L. K. Law, P. A. Wolfgram, D. C. Nobes, M. N. Bone, D. F. Trigg, and J. M. DeLaurier, First results of the MOSES experiment: Sea sediment conductivity and thickness determination, Bute Inlet, British Columbia, by magnetometric off-shore electrical sounding, *Geophysics, 50*, 153–160, 1985.

Flosadóttir, A. H., The response of the oceanic lithosphere to electromagnetic controlled source transmitters using local spectral representation, Ph.D. dissertation, Univ. of Calif., San Diego, 1990.

Fofonoff, N. P., and R. C. Millard, Algorithms for computation of fundamental properties of seawater, *Tech. Pap. Mar. Sci., 44*, 53 pp., UNESCO, Geneva, 1983.

Fraser-Smith, A. C., and D. M. Bubenik, ULF/ELF electromagnetic fields generated above a sea of finite depth by a submerged vertically directed harmonic magnetic dipole, *Radio Sci., 14*, 59–74, 1979.

Fraser-Smith, A. C., D. M. Bubenik, and O. G. Villard, Jr., Large-amplitude changes induced by a seabed in the sub-LF electromagnetic field produced in, on, and above the sea by harmonic dipole sources, *Radio Sci., 22*, 567–577, 1987.

Fraser-Smith, A. C., A. S. Inan, O. G. Villard, Jr., and R. G. Joiner, Seabed propagation of ULF/ELF electromagnetic fields from harmonic dipole sources located on the seafloor, *Radio Sci., 23*, 931–943, 1988.

Inan, A. S., A. C. Fraser-Smith, and O. G. Villard, Jr., ULF/ELF electromagnetic fields generated along the seafloor interface by a straight current source of infinite length, *Radio Sci., 21*, 409–420, 1986.

Kariya, K. A., and T. J. Shankland, Electrical conductivity of dry lower crustal rocks, *Geophysics, 48*, 52–61, 1983.

Kennett, J. P., *Marine Geology*, Prentice-Hall, Englewood Cliffs, NJ., 813pp., 1982.

King, R. W. P., Electromagnetic surface waves: New formulas and applications, *IEEE Trans. Antennas Propag., AP-33*, 1204–1212, 1985a.

King, R. W. P., Electromagnetic surface waves: New formulas and their application to determine the electrical proper-

ties of the sea bottom, *J. Appl. Phys., 58*, 3612–3624, 1985b.

King, R. W. P., and M. F. Brown, Lateral electromagnetic waves along plane boundaries: A summarizing approach, *Proc. IEEE, 72*, 595–611, 1984.

King, R. W. P., J. T. deBettencourt, and B. H. Sandler, Lateral-wave propagation of electromagnetic waves in the lithosphere, *IEEE Trans. Geosci. Electr., GE-17*, 86–92, 1979.

King, R. W. P., M. Owens, and T. T. Wu, Properties of lateral electromagnetic waves and their application, *Radio Sci., 21*, 13–23, 1986.

Kraichman, M. B., *Handbook of Electromagnetic Propagation in Conducting Media*, U.S. Government Printing Office, Washington D.C., 1970.

Levitus, S., Climatological Atlas of the World Ocean, *Prof. Pap. 13*, 173 pp., Natl. Oceanic and Atmos. Admin., Boulder, Colo., 1982.

Mackie, R. L., B. R. Bennett, and T. R. Madden, Long-period magnetotelluric measurements near the central California coast: A land-locked view of the conductivity structure under the Pacific Ocean, *Geophys. J., 95*, 181–194, 1988.

Mott, H., and A. W. Biggs, Very low frequency propagation below the bottom of the sea, *IEEE Trans. Antennas Propag., AP-11*, 323–329, 1963.

Nobes, D. C., L. K. Law, and R. N. Edwards, The determination of resistivity and porosity of the sediment and fractured basalt layers near the Juan de Fuca Ridge, *Geophys. J. R. astron. Soc., 86*, 289–318, 1986.

Oldenburg, D. W., K. P. Whittall, and R. L. Parker, Inversion of ocean bottom magnetotelluric data revisited, *J. Geophys. Res., 89*, 1829–1833, 1984.

Pan, W., Surface wave propagation along the boundary between sea water and one-dimensionally anisotropic rock, *J. Appl. Phys., 58*, 3963–3974, 1985.

Parker, R. L., Understanding inverse theory, *Annu. Rev. Earth Planet. Sci., 5*, 35–64, 1977.

Raemer, H. R., *Statistical Communication Theory and Applications*, Prentice-Hall, Englewood Cliffs, N.J., 482pp., 1969.

Shankland, T. J., and H. S. Waff, Conductivity in fluid-bearing rocks, *J. Geophys. Res., 79*, 4863–4868, 1974.

Spudich, P., and J. A. Orcutt, Petrology and porosity of an oceanic crustal site: results from wave form modeling of seismic refraction data, *J. Geophys. Res., 85*, 1409–1434, 1980.

Tucholke, B. E., N. T. Edgar, and R. E. Boyce, Physical properties of sediments and correlation with acoustic stratigraphy, *Initial Rep. Deep Sea Drill. Proj., 35*, 229–249, 1976.

Wait, J. R., On anomalous propagation of radio waves in Earth strata, *Geophysics, 19*, 342–343, 1954.

Wait, J. R., Electromagnetic propagation in an Earth crust waveguide, *Radio Sci., 1*, 913–924, 1966.

Wannamaker, P. E., J. R. Booker, A. G. Jones, A. D. Chave, J. H. Filloux, H. S. Waff, L. K. Law, and C. T. Young, Conductivity cross section through the Juan de Fuca subduction system and its tectonic implications, *J. Geophys. Res., 94*, 14127–14144, 1989.

Webb, S. C., S. C. Constable, C. S. Cox, and T. K. Deaton, A seafloor electric field instrument, *J. Geomagn. Geoelectr., 37*, 1115–1129, 1985.

Wheeler, H. A., Radio-wave propagation in the Earth's crust, *J. Res. Natl. Bur. Stand., Sect. D, 65*, 189–191, 1961.

Young, P. D., and C. S. Cox, Electromagnetic active source sounding near the East Pacific Rise, *Geophys. Res. Lett., 8*, 1043–1046, 1981.

A. D. Chave, AT&T Bell Laboratories, Room 3L401, 600 Mountain Ave., Murray Hill, NJ 07974.

C. S. Cox and A. H. Flosadóttir, Scripps Institution of Oceanography, A-030, La Jolla, CA 92093.